Investigation of the Microstructure and Mechanical Properties of an Al/SiC/ZrO$_2$ Hybrid Composite by Spark Plasma Sintering Technique

Kalaimani MANIARASU [iD], Shaafi TAJUDEEN* [iD]

Department of Mechanical Engineering, Saveetha School of Engineering, Saveetha Institute of Medical and Technical Sciences, Chennai, India

Highlights
• The spark plasma sintering technique is used to produce the aluminum hybrid composite materials.
• A comparative study of composite material and hybrid composite material.
• Analysis of the material characterization and mechanical properties of hybrid composite materials.

Abstract

Nowadays, aluminum hybrid composite material usage is increasing as a result of a wide range of industrial applications. In the current study, the microstructure and mechanical properties of the Al/SiC/ZrO$_2$ hybrid composite are analyzed using the spark plasma sintering process. In this paper, the weight percentages of primary and secondary reinforcement of SiC and ZrO$_2$ were taken as 5% and 5%, 10% and 15% respectively, for fabrication purposes. The aluminum composite material reinforced with 5% w/w of SiC particles was compared with the aluminum hybrid composite material reinforced with SiC and ZrO$_2$ nanoparticles. The test results show a uniform distribution of the reinforcements due to the fine densification of all the samples. The yield strength, elongation, hardness and compressive strength were decreased by 38%, 1.1% and increased by 32%, 12% respectively in the S4 hybrid composite material when reinforcement particles are added to the composite material, resulting in it being distinctive from the S1 sample. Ultimately, the presence of ZrO$_2$ reinforcements improves the microstructure, microhardness, yield strength, elongation, and compression strength of the aluminum hybrid composite.

1. INTRODUCTION

Structural materials are required to be hard, lightweight and significant influence in the automotive and aerospace sectors. Aluminum is a soft material that is unsuitable for many automotive and aerospace structural components due to its lack of strength and hardness [1,2]. The mechanical, electrical and other qualities of monolithic aluminum structures are currently being improved through research and development based on aluminum composite materials [3,4]. Ramnath et al. [5] compared to conventional construction material, the wear, creep, specific strength, stiffness, and fatigue characteristics are enhanced by the addition of reinforcement to the metal matrix. Aluminum and its alloys serve primarily as matrix materials during the fabrication of composites. The performance of hybrid materials is significantly influenced by their decision of reinforcing materials and the reinforcing particles are associated to the processing parameters. A few distinct reinforcing particle combinations have been taken into consideration while designing aluminum hybrid composites. A comprehensive overview of the production process uses various combinations of reinforcing materials for aluminum matrix hybrid composites and their effects, such as mechanical, corrosion, and wear resistance [6,7]. Combining an aluminum matrix with primary and secondary reinforcing particles to produces the hybrid composites. The incorporation of reinforcement will enhance the material's thermal, chemical, tribological, structural, and other qualities [8,9]. Muley et al. [10] examined the advancements in metal matrix composites based on aluminum, both hybrid and nanoscale. They concluded that hybrid aluminum matrix composites have superior characteristics to single-reinforced aluminum composites. Materials with increased strength, improved wear resistance, and reduced weight are now required by the automobile industry. In this regard, Chandel et al. [11] studied and concluded that the hybrid composite has a high potential to replace aluminum alloy with primary reinforcing composite

---
*Corresponding author, e-mail: shaafit.sse@saveetha.com

material in an automotive industry. To maximize the material attributes, the primary and secondary hybrid composite material reinforcements properties can be changed.

By strengthening the aluminum matrix with a variety of ceramic particles and volume ranges, a large number of materials science and engineering researchers are working on to enhance the mechanical characteristics of composites. Inegbenebor et al. [12] Using the stir casting method, SiC was used to strengthen the aluminum matrix at different weight ranges of 2.5%, 5.0%, 7.5%, and 10%. In comparison to (29 μm) silicon carbide, the authors reported that a 7.5% volume fraction of (3 μm) silicon carbide produced higher values for Young's modulus (E) and hardness, with values of 1517.6 MPa and 26.1 Hv, respectively. Liu Zhang et al. [13] investigated the impact of different B_4C volume contents (5%, 10%, 15%, 20%, and 25%) reinforced by matrix composites made using the vacuum heating-press sintering process. The study focuses on the microstructure, phase composition and mechanical characteristics of the Al/B_4C composition. The researchers additionally reported a maximum of 99.22% and 54.63±7.43%, respectively, for 5 vol% B_4C/Al composites. The researchers concluded that ductility and relative density consistently increased as the volume of aluminum increased. The mechanical and tribological characteristics of the AMMCs (2–10 wt%) of TiC were investigated under both heat-treated and cast conditions. The authors [14,15] observed that, in comparison to the cast condition, the mechanical and tribological characteristics of the T_6, matrix, and composite were better under the under-heat-treated conditions. Similarly [16,17], using a hot extrusion technique with microwave-assisted powder metallurgy, Al_2O_3 composites reinforced with volume percentages of 5, 10, and 15% Al_2O_3 were created. In comparison to the Al matrix, the further extruded state shows greater tensile strength at high temperatures. This Al-15 vol.% Al_2O_3 composite yields ultimate tensile and yield strength.

Aktaş et al. [18] produced the $AlZrO_2$ nanocomposites using nanopowders of aluminum and ZrO_2 reinforced particles through the hot pressing method combined with a mechanical milling process, further evaluating the microstructure, physical and mechanical properties of unreinforced aluminum and $AlZrO_2$ nanoparticles. The authors found that the $AlZrO_2$ nanoparticles have better compressive strength, hardness and increased porosity, but at the same time the compressive strength of $AlZrO_2$ was decreased due to the clustering of nano ZrO_2 reinforced particles and the reduced densification of the powder particles. Abdo et al. [19] examined the developments of Al-ZrC nanocomposites produced by adjusting the weight percentage of reinforcement using the spark plasma sintering technique and the obtained results exhibit better load-carrying ability due to the thermal mismatch between Al and ZrC, which causes a reduction in grain size, homogeneous dispersion of reinforcing particles, and dislocation. Al-based hybrid composites wear and microhardness characteristics were investigated by [20] as a function of TiO_2 concentration at 0%, 4%, 8% and 12% mass fractions using the powder metallurgy (P/M) method and the results obtained indicated that when the TiO_2 concentration increased, wear resistance and microhardness also increased.

Chen et al. [21] formed the in situ composites (Al-matrix, TiB particles of 10-50 μm size and 10 vol%) made by the stir casting process without secondary processing such as extrusion. The authors have noticed that T_6 heat treatment exhibited a modulus of 91 GPa, an excellent tensile strength of 270 MPa, and 8% ductility. Meena et al. [22] used the melt-stirring technique to determine the mechanical properties of Al-6063 metal matrix composites along by silicon carbide reinforcements. They varied the weight percentage of the reinforced particles, which varied from 5%, 10%, 15%, and 20%, with different sizes of mesh (220, 300, and 400). The study revealed that the tensile strength, hardness, and impact strength exhibited a positive correlation with the increase in the reinforced weight fraction. Karvanis et al. [23] studied the mechanical characteristics such as hardness, tensile, compressive and drop-weight impact strength of Al-SiC with varying amounts of carbide using a centrifugal casting machine. The authors found that the Al-SiC composites enhanced both tensile and compressive strength by increasing the percentage (3, 6, 9, 12 and 15%) of silicon carbide. Surya et al. [24] concentrated on using powder metallurgy to create functionally graded materials and studying their mechanical properties. Due to its brittle nature, SiC makes composites difficult to machine; nevertheless, the inclusion of metal oxides alters SiC's brittleness and expands its range of engineering uses. Raghuvaran et al. [25] Researchers looked at the mechanical characteristics of the Al7075-SiC composite material and found that adding 6% of SiC made the tensile strength and hardness values go up. However, adding more than 6% of SiC made the wear rate go down and the tensile strength and hardness values go down.

Rajasekaran et al. [26] investigated the mechanical properties characterized before and after the thermomechanical treatment of the silicon carbide particles with Al7075. The test result shows that: (i) 5% of the SiC hardness value was improved by more than 20% (ii) 7.5% and 10% of SiC the hardness value was 10%. Şimşek et al. [27] conducted the studies on AMC material with different amount of ZrO_2 to the AlGr matrix. The authors concluded that, increases the ZrO_2 in the matrix, has increasing the order of hardness and density. Using the stir casting process, A356 aluminum alloy composites reinforced with ZrO_2 have been produced by adjusting the casting temperature to 750°C, 850°C and 950°C. [28] observed that adding 15% ZrO_2 particles to the A356 matrix alloy increased its ultimate strength and hardness. The aluminum extrusion AA6063 experiment was carried out by Dhandapani [29]. Metal matrix composites (MMC) reinforced with 5, 10, and 15% vol% ZrO_2 were made at three different casting temperatures (750, 850, and 950°C) using the stir casting process. Adding ZrO_2 particles made the Al matrix extrusion 70 BHN tougher and increased its ultimate tensile strength by 232 MPa. Thus, the specimen that included 15% ZrO_2 and was created at 750°C had the best mechanical properties.

Naveen Kumar et al. [30] examined the aluminum alloy's tribological and mechanical properties with the effect of nanosized monometallic zirconium dioxide particles. James et al. [31] invented the hybrid matrix composite comabining both ZrO_2 and Al_2O_3 as reinforcement for Al6061 matrix and the authors conluded that Al6061 has higher tensile strenght than base alloy Al6061. The mechanical and tribological properties of hybrid composites material enhanced with ZrO_2 nanoparticles and SiC microparticles based on aluminum were prepared by powder metallurgy and then investigated by [32], and the authors reported that the Al-5%SiC-9%ZrO_2 hybrid composite was preferred for high wear resistance applications. Khan et al. [33] studied the mechanical properties of Al-SiC-ZrO_2 nanocomposites with varying ZrO_2 concentrations (3, 6, and 9 wt.%) and a constant amount of SiC (5 wt.%). When compared to Al and other composites, the results show that Al-SiC-ZrO_2 nanocomposites with 9 wt.% ZrO_2 nanoparticles have excellent yield, compressive strength, and hardness. The research findings of novel materials synthesized using spark plasma sintering (SPS) process with plasma spark mechanisms. Moreover, the authors [34] emphasized the characteristics of the product, which include materials that are difficult to sinter, materials that include corban, materials that are nanocrystalline, materials that are not in equilibrium, gradient materials, materials that link, materials with complicated shapes, and advanced functional materials.

Aluminum hybrid composite materials are prepared by different processes, such as liquid, solid, powder and other processes. The powder state process of spark plasma sintering has been widely used among the other processes. There is a very limited work on using the spark plasma sintering process for aluminum hybrid composites. The objective of this study was to conduct a comparison of the mechanical properties and synthesis of aluminum hybrid composites made with the spark plasma sintering technique to the Al/5 w/w.% SiC composite material. The study also examined the effects of varying the concentrations of ZrO_2 (5%, 10%, and 15% w/w.%).

2. EXPERIMENTAL METHODS

2.1. Material Preparation

In this work, hybrid nanocomposites were created with various ZrO_2 particle reinforcements using pure aluminum as the foundation material for the spark plasma sintering technique. Table 1. shows the chemical element composition of pure aluminum. It acquired the pure aluminum, SiC, and ZrO_2 from M/s Ultra Nanotech, located in Bangalore, India, with particle sizes of 30 - 50 μm, 30 - 50 nm and 30 - 50 nm respectively. The required samples denoted as S1, S2, S3 and S4 were taken with the desired weight percentage of reinforcement particles. At room temperature, the powder mixtures were blended using a planetary mono mill pulverisette 6 classic line tester shown in Figure 1, where used for a period of one hour at a milling speed equal to 150 rpm. This was done to make sure that the ceramic particles were distributed evenly throughout the mixtures. Five 5mm-diameter tungsten carbide balls were used to assist combine the particles. After the removal of the ground powder from the ball mill process, green compaction was performed at a pressure of 40 MPa using an SPS graphite mould that had the right form. Table 2. displays the samples composition ratio.

Figure 1. *Shows planetary mono mill pulverisette 6 classic line*

Table 1. *Chemical element composition of pure aluminum*

Elements	Si	Fe	Cu	Mn	Zn	Sn	Ti	Cr	Al
Wt.%	0.02	0.03	0.006	0.001	0.025	0.030	0.004	0.003	99.88

Table 2. *The composition ratio of samples Al/SiC/ZrO$_2$ hybrid composite*

S.No.	Samples Name	Compositions	References
1	S1	Al - 5 w/w.% SiC	[19,20]
2	S2	Al - 5 w/w.% SiC - 5 w/w.% ZrO$_2$	[25]
3	S3	Al - 5 w/w.% SiC - 10 w/w.% ZrO$_2$	[26]
4	S4	Al - 5 w/w.% SiC - 15 w/w.% ZrO$_2$	[23, 25, 26]

The SPS process was used to introduce each green compaction sample, as shown in Figure 2. Utilize a vacuum technique to extract gases from the punches, mould, and spark plasma chamber. Following that, apply a pressure of 30 MPa, and then perform the execution of the resistance heating vacuum process. During the sintering process, the different polarity of the pulsed direct current (DC) was supplied through the punches and the plasma spark was generated between the powder particles. The melted regions are fusing, creating connections between the powder particles through use of electron current (during the ON time) and vacuum generation (during the OFF time). Based on Figure 3. the spark plasma process generated heat in the mould and punch, leading to a temperature rise to 600°C at a pressure of 30 MPa. Using compressive force in the SPS method improved the bonding between particles in the samples, which made the powder particles stick together better. Samples of hybrid composite materials with different ranges of reinforcement compositions, labeled S1, S2, S3, and S4, were obtained. These samples had dimensions of 100 mm in length and 25 mm in diameter.
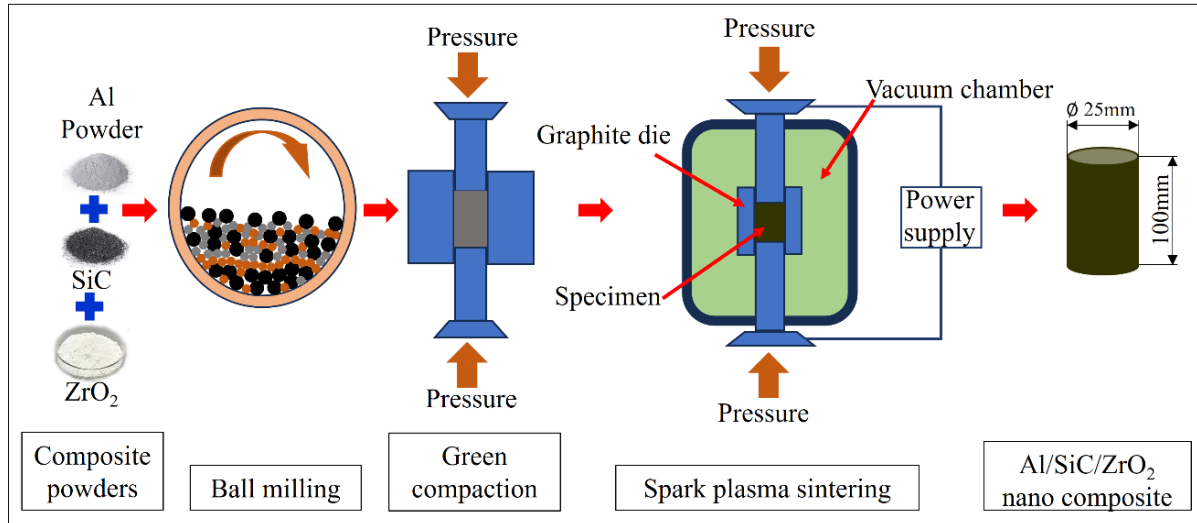
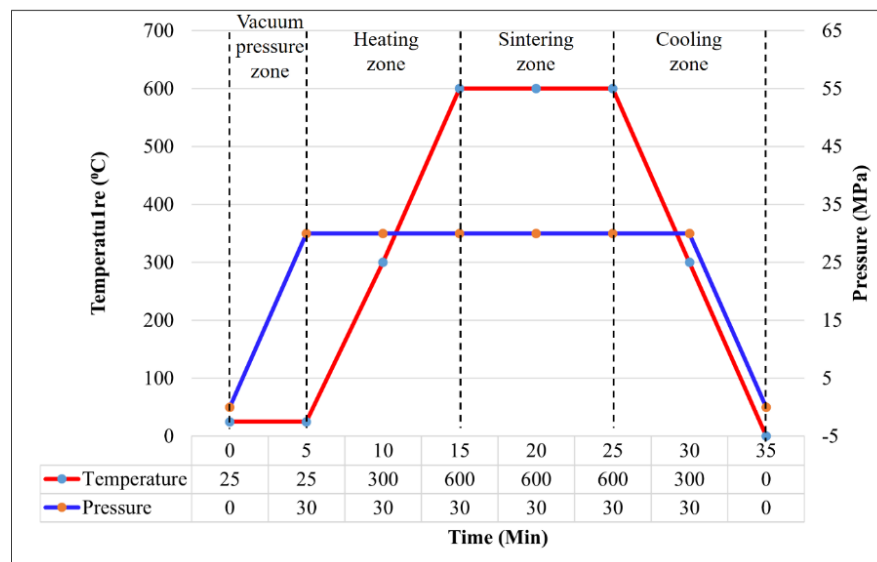*Figure 2. Schematic diagram of spark plasma sintering (SPS) process*

Figure 3. Shows the spark plasma process time Vs pressure, temperature

2.2. Material Characterization

2.2.1. X-Ray diffraction

An X-ray diffraction analysis was performed on the aluminum hybrid composites of samples (S1, S2, S3, and S4) using the PANalytical X-Pert Pro MRD with a resolution of 0.0001°/0.36 arcsec, The Netherland. The range of 20° to 80° in 2θ was used to record the analytical peak intensities.

2.2.2. Density

Using an electronic weighing equipment with a density calculation function, the Archimedes principle may be used to quantitatively calculate a composite's experimental density (ρ_{Exp}) with the ASTM: D 792-66 test procedure [35]. The density was determined to all the samples S1, S2, S3 and S4. For explaining the testing procedure was followed in the sample S4 mass of 150g was determined through the process of weighting the aluminum hybrid composite using a digital scale. Volume was determined for the sample using a graduated glass vessel filled with water after obtaining the mass. A reading of 300 ml was initially recorded. Following this, the hybrid composite was submerged in the vessel filled with water, and the resulting rise in water level was measured to be 354 ml, which corresponds to the final water level. In

centimetres, the volume of the hybrid composite sample S4 is obtained by subtracting the initial water level from it. The result was 54 ml, using the mass and volume values specified in Equation (1), the density of the sample S4 of the hybrid composite was determined to be 2.78 g/cm³

$$Experimental\ density\ (\rho_{Exp}) = \frac{mass\ (g)}{volume\ (cm^3)}. \tag{1}$$

Equation (2) [36], express the theoritical density (ρ_{Th}) of the hybrid composite. The mass fraction of pure aluminum (m_{Al}), silicon carbide (m_{SiC}) and zirconium dioxide (m_{ZrO_2}) respectively. Also, the density of aluminum ($\rho_{Al} = 2.7g/cm^3$), silicon carbide ($\rho_{SiC} = 3.21g/cm^3$) and zirconium dioxide ($\rho_{ZrO_2} = 5.68g/cm^3$) respectively

$$Theoritial\ density\ (\rho_{Th}) = (m_{Al}\% \times \rho_{Al}) + (m_{SiC}\% \times \rho_{SiC}) + (m_{ZrO_2}\% \times \rho_{ZrO_2}). \tag{2}$$

In order to determine the porosity of samples S1, S2, S3, and S4 by using the Archimedes method of procedure as followed by the Equation (3)

$$Porosity\ (\%) = \left(1 - \frac{\rho_{Exp}}{\rho_{Th}}\right) \times 100. \tag{3}$$

2.2.3. Microhardness

The microhardness test measures the hardness of small sample parts (S1, S2, S3 and S4) using a Shimadzu brand HMV-2 model Vicker hardness testing machine (ASTM E384) at room temperature [35,37]. The test was performed by the pressing a standard indenter with a particular shape into the test material surface at a test load of 500 gf (4.90 N) and the hold time is 10 seconds. Then optically measuring the indentation of diagonals (d_1 and d_2) and as on three indentation test conducted for each samples. The micro hardness value is calculated by the Equations (4) and (5) [38]. Where *HVN* is vicker hardness number (Vicker unit), *d* is the average diagonal length (mm) value, and *F* is the test load (gf)

$$HVN = 1854.4 \times \frac{F}{(d^2)} \tag{4}$$

$$d = \frac{d_1 + d_2}{2}. \tag{5}$$

2.2.4. Yield strength

The yield strength test was conducted on the aluminum hybrid composite samples (S1, S2, S3 and S4) on the computerized servo hydraulic universal testing machine (UTM) as per the ASTM E-8-04 standard show in Figure 4 [35,39] at a room temperature 30°C. The gauge length of the specimen is set at 25 mm, while the crosshead speed is maintained at 2.5 mm/min. These parameters have been carefully selected to accurately determine the yield strength. All the original lengths of the test samples were measured and fixed between the upper and lower jaws of the UTM machine. In the operation, the upper jaw moves in an upward direction to increase the tension force at a specified crosshead speed. This force was applied up to the end of the hybrid composite's elastic region, which is used to calculate the samples yield strength. the elastic region of the hybrid composite to determine the yield strength of the samples. After completion of the yield strength test, the samples were collected and the final elongation length of each sample measured. Every sample final elongation length to original length difference was calculated to determine the percentage of elongation for all samples.
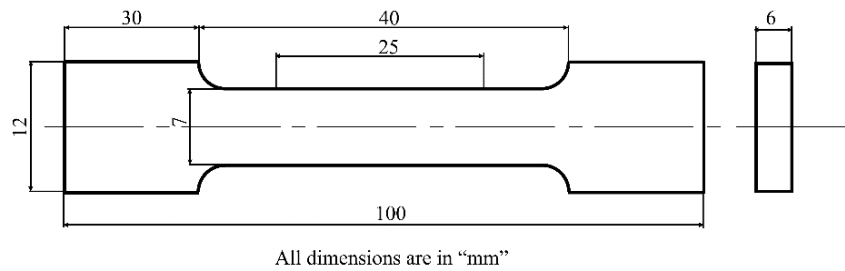
Figure 4. *ASTM E-8-04 standard tensile test specimen*

2.2.5. Compression strength

The aluminum hybrid composite was subjected to a tensile test sample (S1, S2, S3 and S4) on the computerized servo hydraulic universal testing machine (UTM) as per the ASTM E9-09 standard [37,40] at a room temperature of 30°C. The test samples were placed between two flat plates and tested for compressive force in order to determine the maximal failure stress throughout the testing procedure. The crosshead speed of 1 mm/min was utilised during the measurement. For the compressive test, the samples was produced with a 20 mm diameter and a 40 mm length.

## 3. THE RESEARCH FINDINGS AND DISCUSSION

3.1. XRD Analysis

Figure 5 shows the XRD patterns of the hybrid Al/SiC/ZrO$_2$ composite. The sample S1 shows the compositions of Al and 5w/w.%SiC concentration was enhanced in the intensities peak. The high intensities peaks appeared on $2\theta = 34°$ and realted peaks are $2\theta = 42°, 60°$ and $70°$ respectively, the equivalent SiC planes 111, 200, 220, and 311, in that order. The notable peak intensities appeared, further increasing the reinforcement of ZrO$_2$ in the samples S2, S3 and S4 respectively. The main peaks observed at $2\theta = 31°$ and the small peaks appeared at $2\theta = 51°, 64°$ and $75°$ respectively, corresponding to the 200, 202 and 220 planes of ZrO$_2$ respectively (JCPDS No. 89-9066) [41].

Figure 6 displays the X-ray diffraction (XRD) results for sample S4. The study of pure aluminum (Al) shows that the peaks at miller indices 111, 200, 220, and 311 are in line with certain crystallographic planes in aluminum face-centred cubic (FCC) structure. The peaks denoted as (111), (200), (220), and (311) respectively, indicate reflections occurring from the lattice plane, the 200, 220, and 311 planes respectively [37]. The discernible interplanar spacings between these planes within the FCC crystal lattice enhance the characterization of the structural properties of the material.

The silicon carbide (SiC) exhibits characteristic peaks 111, 200, 220, and 311, indicative of its crystalline structure.The reflectance from the 111 lattice plane is denoted by the (111) peak, the intensities of peak (200), (220) and (311), all of which are associated with the hexagonal crystal lattice of SiC. The XRD spectrum exhibits visible peaks that furnish critical insights into the atomic arrangement within the crystal lattice of SiC (JCPDS 29-1129) [42].

The distinct peaks 101, 200, 202, and 220 of the zirconium dioxide (ZrO$_2$) provide significant information on its crystallographic structure. Depending on the phase stability, the (101) peak corresponds to the reflection from the lattice plane, (200) represents the plane, (202) is associated with the plane, and (220) represents the plane in the cubic crystal lattice of ZrO$_2$.
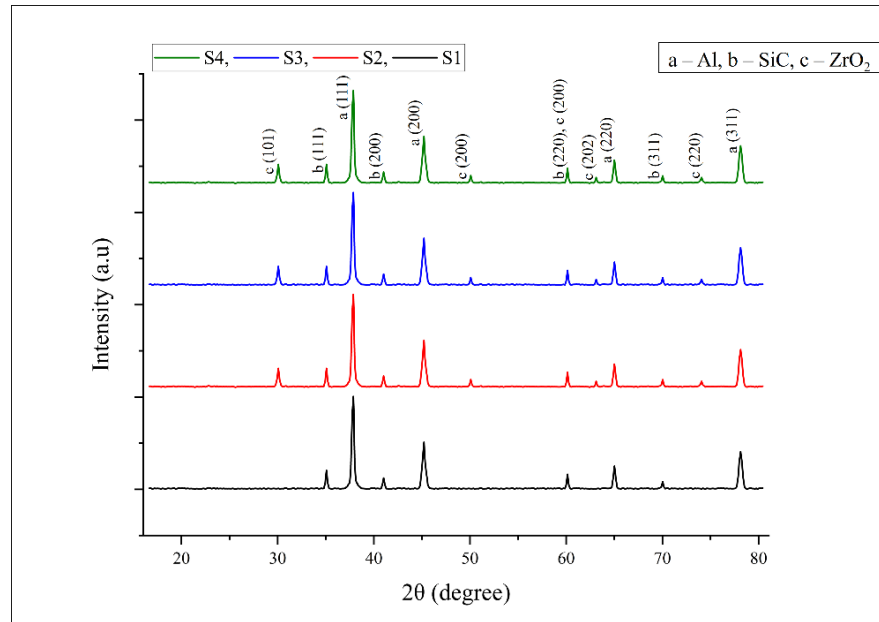
**Figure 5.** *Shows the hybrid Al/SiC/ZrO$_2$ composite of XRD patterns*
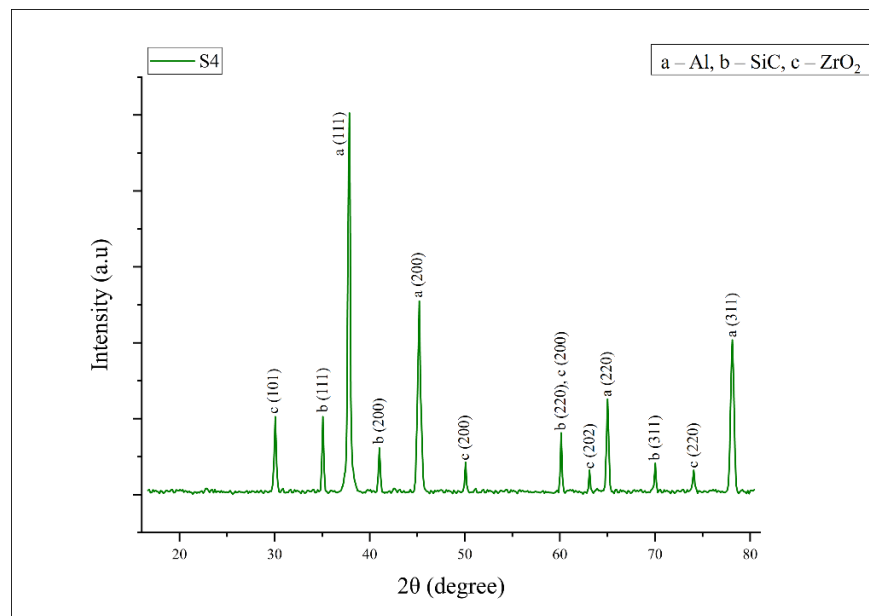
**Figure 6.** *XRD pattern for sample S4*

3.2. Microstructural Analysis

The misconstrue shows a homogeneous distribution of small pores for the samples S1, S2, S3 and S4. In addition, with the increasing ZrO$_2$ content, the crystalline structure of the sintered composites becomes finer, with refined grains observed in the composites containing ZrO$_2$ and SiC particles along the grain boundaries. Additionally, it is observed that the presence of ZrO$_2$ reduces the number of pores [33]. The characteristics of hybrid composite are determined by the weight percentage, the metal matrix, the particle reinforcement arrangement, and the adhesion at the interface between the particles and the matrix. Additionally, it is observed that the area fraction increases in proportion to the weight percentage of ZrO$_2$ reinforcement [43]. The scanning electron microscopic image for spark plasma sintered hybrid composites with different reinforcements is shown in Figure 7. The reinforcements of SiC and ZrO$_2$ are uniformly dispersed throughout the Al base material with minimal agglomeration in the sample S3. Manvendra Yadav et al. [44] The study found that the Al/10%ZrO$_2$ metal matrix composite showed micron-sized ZrO$_2$

agglomerated precipitates that were unevenly dispersed. The formation of the Al/ZrO_2 composite was responsible for the whitish contrast region observed. The hybrid composites microstructure and mechanical properties are significantly influenced by the uniformity and amount of ZrO_2 within the aluminum matrix. The SEM images of Al exhibit the bonding strength due to the presence of ZrO_2 and SiC which were consistent in the presence of reinforcements.
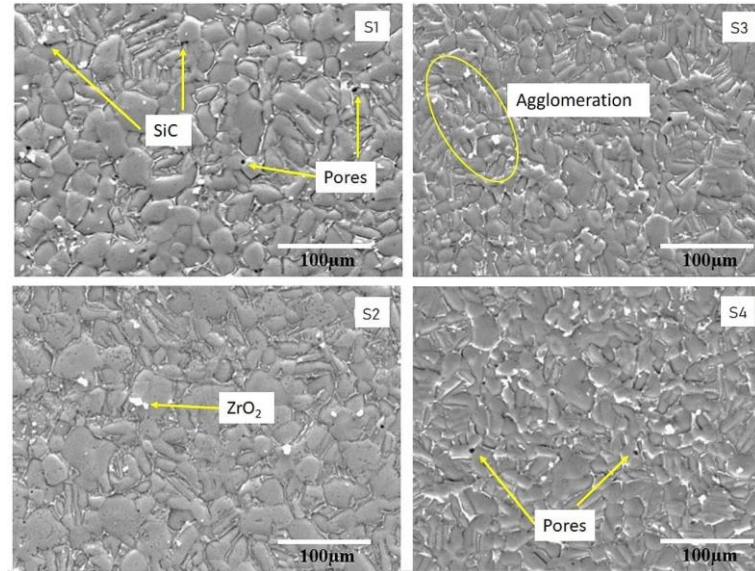
Figure 7. *SEM Images of, (S1). Al – 5w/w.% SiC, (S2). Al – 5w/w.% SiC – 5w/w.% ZrO₂, (S3). Al – 5w/w.% SiC – 10w/w.% ZrO₂, (S4). Al – 5w/w.% SiC – 15w/w.% ZrO₂*

3.3. Energy Dispersive X-Ray Spectroscopy (EDX)
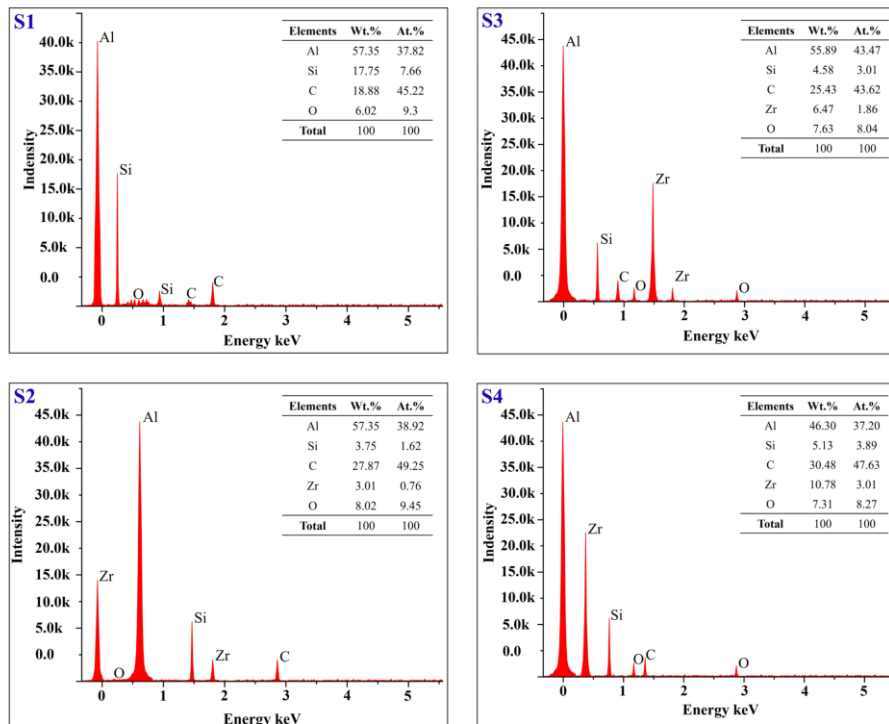
Figure 8. *Shows that the energy dispersive X-ray spectroscopy (EDX) analysis result*

EDX is able to develop the most suitable approaches for micro- and nano-characterization and that is necessary in cases where primary and secondary reinforcement of the structural features is needed. This makes the analysis more precise and accessible. Figure 8 shows that the EDX analysis result proves the reinforcement and unit percentage. Composites of the aluminum matrix may be seen in the EDX pattern as particles of SiC and ZrO_2 are dispersed throughout the material. The elements Si and C indicate the presence of SiC reinforcement on the S1 samples and the elements Zr and O indicate the presence of reinforcement of ZrO_2 on the samples S2, S3 and S4. The primary reinforcement element of Si and C presence was increased in the samples of S2, S3 and S4. On the other hand, when SiC reacts with aluminum and Si elements bond with aluminum, the C element increases in all four samples. However, the secondary reinforcement of ZrO_2 reacts with aluminum and the Zr element increases gradually with w/w.% and the O element reacts with aluminum to form the oxide layer on the materials.

3.4. Density

The densities of Al, SiC and ZrO_2 are 2.7 g/cm^3, 3.21 g/cm^3 and 5.68 g/cm^3 respectively. The relative density and porosity of the hybrid composite with different reinforcements are shown in Figure 9. Theoretical density and the experimental density of the composite were calculated using the mixing procedure and the Archimedes principle [45]. The density was decreased with the addition of the reinforcement w/w.% ZrO_2 for S2, S3 and S4 as compared with the S1 sample reinforced with Al/5% SiC and the similar results were noticed by [46] for their aluminum Al7075 alloy reinforced with ZrO_2 particles, The experimental density was comparatively low compared to the theoretical density among the samples S1, S2, S3 and S4 respectively. Even though the sample S2 had two different reinforcement particles of 5w/w.% of SiC and 5w/w.% of ZrO_2 as compared to the sample S1, single reinforcement particles of 5w/w.% of SiC are also close to the same value in the experimental density value. The experimental density of the sample S4 was decreaed by 0.1 g/cm^3 with the reinforcement of Al/5w/w.%SiC/15w/w.%ZrO_2 as compared with the sample S1 reinforced with Al/5w/w.%SiC.
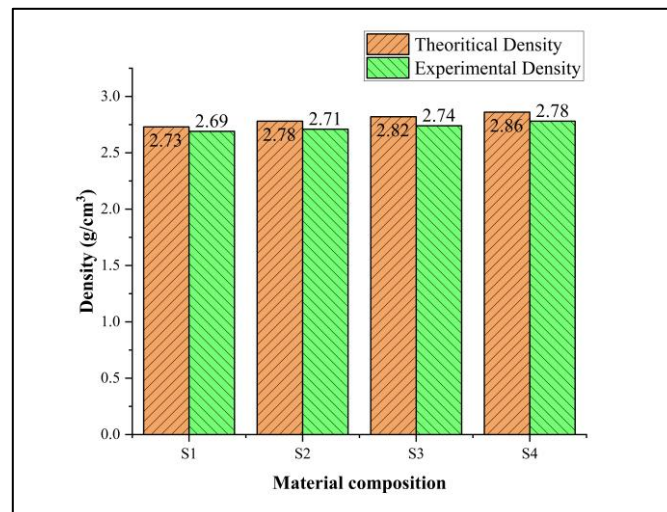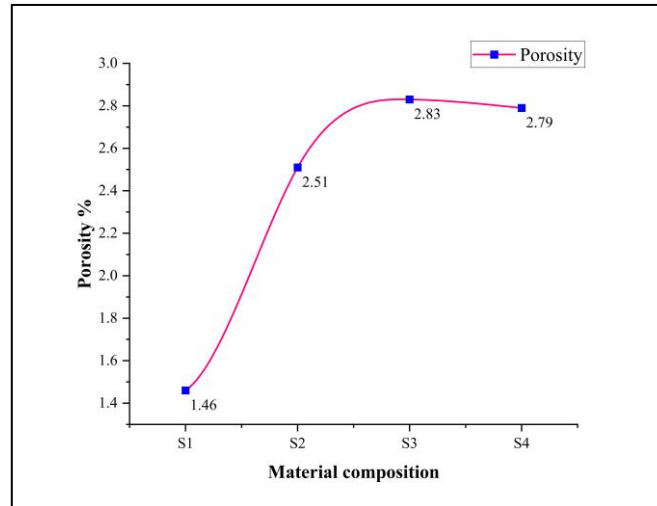

Figure 9. *Shows the variations of sintered density with different samples*

3.5. Porosity

Figure 10 shows the porosity of the hybrid composite materials of the prepared samples. The minimum porosity of the S1 sample seems to be low by 1.46% and the maximum porosity by 2.79% for S4 sample. The SEM image of the S4 sample shows the very minimum porosity as compared to the S1 sample due to increasing the ZrO_2 reinforcement particles, as its reflection in the porosity figure shows the S4 sample decreased the porosity by 2.79% compared to the sample S3 porosity of 2.83%. The porosity of S4 sample was increased by 1.33% when comparing the composite materials of the S1 sample, there are noticeable differences. Porosity can be formed into aluminum hybrid composites through the powder metallurgy procedure. Particle size, distribution, and sintering temperature are the primary determinants of the

formation of pores in a material, which subsequently influence its microhardness and other mechanical properties. The local stress concentration may occur in pores, resulting in a decrease in microhardness in those specific areas. During the sintering process, an increase in temperature over a 15-minute period leads to a corresponding increase in porosity. When the sintering temperature decreases from 15 to 35 minutes, the porosity will decrease during the sintering process [47].

Figure 10. Shows the variations of sintered porosity with different samples

3.6. Microhardness

The microhardness of the hybrid composite shows a clear improvement as ZrO_2 particles are slowly added, showing a significant improvement compared to the base S1 sample composite material, as shown in Figure 11. Specifically, adding reinforcements with 5%, 10%, and 15% w/w.% of ZrO_2 to samples S2, S3, and S4 makes them harder, as measured by *HVN* values of 65, 78, and 84 respectively. The findings indicate that the reinforcing particles are of vital importance in strengthening the composite structure, thereby enhancing its mechanical properties and resistance to indentation [48]. The corresponding increase in microhardness is proof of the connection between the hybrid composite material hardness characteristics and the incremental nature of the reinforcement.
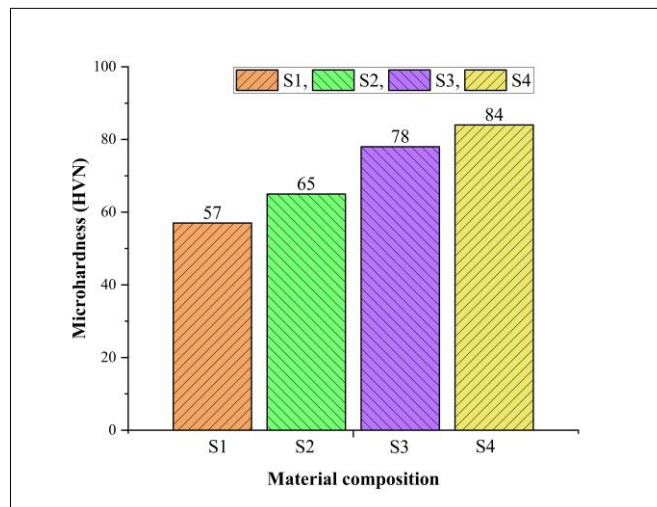
Figure 11. Shows the microhardness of hybrid composite materials

3.7. Yield Strength

Figure 12 shows the yield strength of the hybrid composite. The yield load was applied with an elastic limit to measure the yield strength of the prepared samples. The experiment proves that when the weight percentage of the ZrO_2 particles increase as it simultaneously increases the hardness of hybrid composite materials, but at the same time, increasing the hardness decreases the yield property of hybrid composite material. The hard ceramics of ZrO_2 nanoparticles and their capacity to prevent matrix deformation and contributed towards the improvement of hardness. The yield strength of the S4 sample was reduced (70 MPa) when compared to the S1 sample (114 MPa).
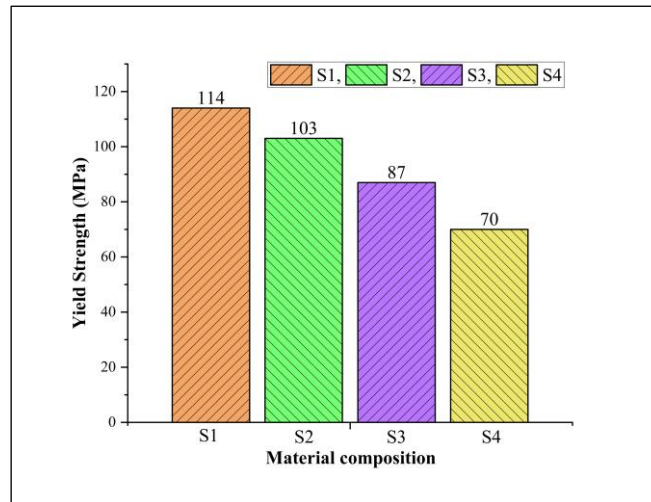
Figure 12. Shows the yield strength of the hybrid composite materials

3.8. Elongation

Figure 13 shows the percentage elongation of the hybrid composite. The results indicate that the elongation of the material decreases as the weight percentages of zirconium dioxide are added. The samples indicate as S2, S3, and S4 undergo a transformation from ductile to brittle on their addition of zirconium dioxide. As a result of the addition of zirconium dioxide, the hybrid composite becomes brittle and loses its ductility. The elongation of the S1 sample is decreased by 3.1% upon the addition of zirconium dioxide, a decrease of 2.5%, 2.3%, and 2% respectively and the similar results were noticed by [35]. The sample S4 elongation is reduced to 1.1% when compared to sample S1.
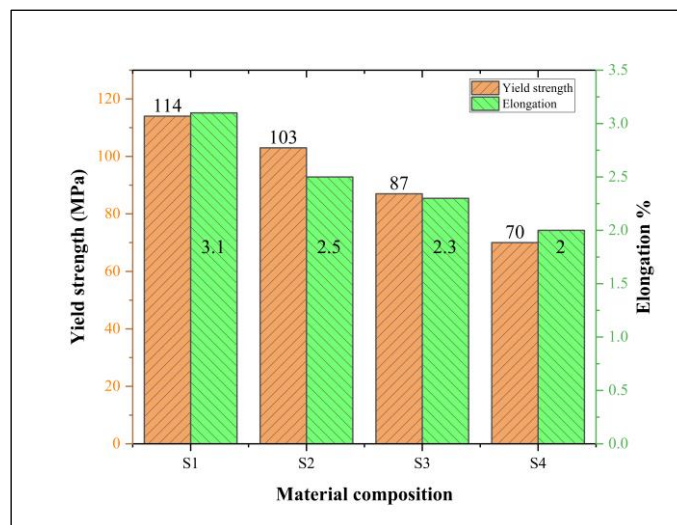
*Figure 13. Shows the elongation of the hybrid composite materials*

3.9. Compressive Strength

The compression test was done by using a universal testing machine (UTM) with the maximum load of the sample at the room temperature. The sample S2, S3 and S4 were gradually increased the maximum compressive strength 354, 372 and 394 MPa respectively. Due to the reinforcements of ZrO_2 particles, it is noticed that the sample S3 and S4 loses the ductility and the transition occurs ductile to brittle material [33]. The enhancement of the hardening function might be attributable to the elastic characteristics of ZrO_2 particles and their ability to prevent matrix deformation. Therefore, when a suitable interface is present, the ZrO_2 particles inhibit matrix deformation and enhance work hardening [49]. It is clear that the ZrO_2 nanoparticles were improved the hybrid composites compressive strength when they were added to samples S2, S3 and S4 due to the following reasons: (i) uniform distribution of hard ceramic ZrO_2 nanoparticles; and (ii) dispersion hardening effect (enrichment of the dislocation density) [50]. The effect of adding ZrO_2 increases the physical hardness of the hybrid composite materials, but on the other hand, it also increases the compressive resistance. The S4 sample has a high compressive strength of 394 MPa, as shown in Figure 14.
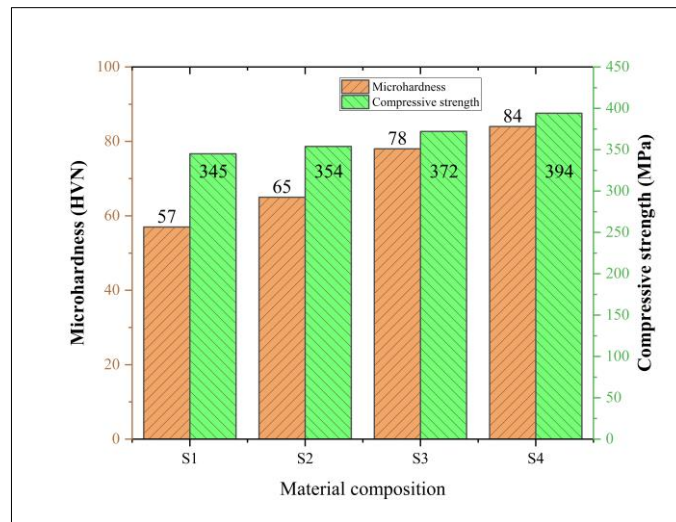
Figure 14. *Shows the compressive test of hybrid composite*

The compressive test reveals that the strength of the aluminium-hybrid composite increases as the weight percentage of the ZrO_2 particles ncreases. The compressive fracture was attained at the maximum load, as shown in Figure 15. The initial compressive loads were applied to the samples and gradually increased, while on the other hand, the grain-particle interface of the samples was dislocated due to the compressive deformation. At the end of the deformation, fracture began on the top side of the samples and was extended by a shear portion diagonally, and on the fracture surface appeared particles shear. The samples S2, S3 and S4 attain brittle fractures with the addition of reinforcement ZrO_2 particles.
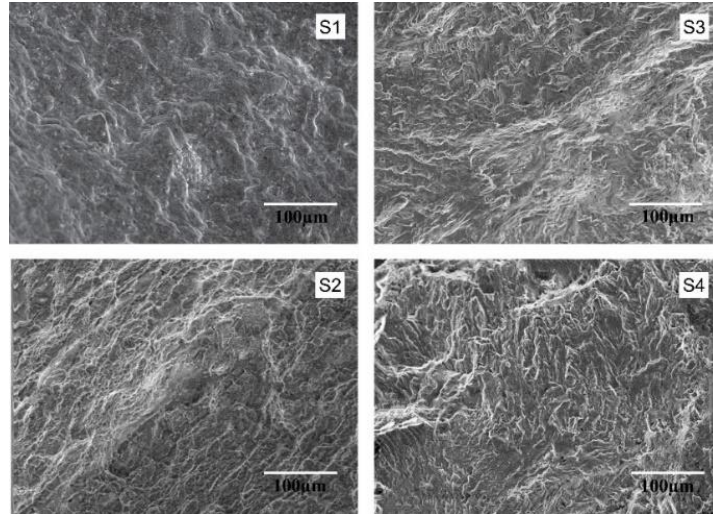
Figure 15. *Shows the compressive test fracture*

4. CONCLUSION

In this paper, the Al/SiC/ZrO$_2$ hybrid composite materials were prepared by the spark plasma sintering technique with constant primary reinforcement of 5 w/w.% SiC varying with secondary reinforcements of ZrO$_2$ (5%, 10% and 15% w/w.%) compared between the hybrid composites of samples S2, S3 and S4 with sample S1 composite material. The following conclusions were reached from the experimental analysis:

- The pore distribution in samples S1, S2, S3, and S4 is uniformly small in microstructure. Sintered composites containing particulates on grain boundaries are refined by increasing ZrO$_2$ content, which reduces porosity. Reinforcements of SiC and ZrO$_2$ are dispersed uniformly throughout Al, with minimal agglomeration in S3. The Al/10% ZrO$_2$ composite exhibits micron-sized ZrO$_2$ agglomerates that are irregularly dispersed, resulting in a whitish contrast. The quantity and uniformity of ZrO$_2$ have an important role in the influence of the microstructure as well as the mechanical characteristics of hybrid composites in the Al matrix. The aluminum hybrid composite exhibits consistent bonding strength in SEM images due to the reinforcements of ZrO$_2$ and SiC.

- The density of the hybrid composite sample S4 was increased by 2.78 gm/cm^3 due to the related properties of the microhardness of sample S4 which improved by 32% when compared to the sample S1 composite material.

- A considerable increase in microhardness is observed in the hybrid composite as ZrO$_2$ particles are incorporated gradually, in contrast to the base S1 sample. More precisely, the hardness of samples S2, S3, and S4 is enhanced by the addition of 5%, 10%, and 15% w/w.% ZrO$_2$, as indicated by *HVN* values of 65, 78, and 84 respectively. The results of this study highlight the critical significance of reinforcing particles in fortifying the composite structure, resulting in enhanced mechanical characteristics and heightened resistance to indentation. The correlation between the increase in microhardness observed in the hybrid composite material provides support for the incremental nature of the reinforcement and its impact on hardness properties.

- In order to determine the yield strength of the prepared samples, a yield load was applied within the elastic limit. Due to the experiment, the hardness of the hybrid composite materials increases proportionally with the weight percentage of ZrO$_2$ particles. An examination of the S4 and S1 samples indicates that the yield strength of the S4 sample (70 MPa) is comparatively lower than that of the S1 sample (114 MPa).

- The results of the compression test indicated that the maximal compressive strengths of samples S2, S3, and S4 increased gradually to 394 MPa, 354, 372, and 374 MPa respectively. The incorporation of ZrO_2 reinforcements resulted in a reduction in ductility for samples S3 and S4, causing a transition in the material's behaviour from ductile to brittle. Significantly, the compressive strength of the S4 sample was 394 MPa, which was considerably higher than the S1 sample 345 MPa.

CONFLICT OF INTEREST

No conflict of interest was declared by the authors.

REFERENCES

[1] Singla, M., Dwivedi, D. D., Singh, L., Chawla, V., "Development of aluminium based silicon carbide particulate metal matrix composite", Journal of Minerals and Materials Characterization and Engineering, 8(06): 455, (2009).

[2] Chatterjee, A., Sen, S., Paul, S., Ghosh, K., Ghosh, M., Sutradhar, G., "Fabrication and characterization of silicon carbide and graphite reinforced aluminium matrix composite", Journal of The Institution of Engineers (India): Series D, 104(2): 587-601, (2023).

[3] Chak, V., Chattopadhyay, H., Dora, T. L., "A review on fabrication methods, reinforcements and mechanical properties of aluminum matrix composites", Journal of Manufacturing Processes, 56: 1059-74, (2020).

[4] Mondal, S., "Aluminum or its alloy matrix hybrid nanocomposites", Metals and Materials International, 27: 2188-2204, (2021).

[5] Ramnath, B. V., Elanchezhian, C., Annamalai, R. M., Aravind, S., Atreya, T. S. A., Vignesh, V., Subramanian, C., "Aluminium metal matrix composites–a review", Reviews on Advanced Materials Science, 38(5): 55-60, (2014).

[6] Bodunrin, M. O., Alaneme, K. K., Chown, L. H., "Aluminium matrix hybrid composites: a review of reinforcement philosophies; mechanical, corrosion and tribological characteristics", Journal of Materials Research and Technology, 4(4): 434-445, (2015).

[7] Lakshmikanthan, A., Angadi, S., Malik, V., Saxena, K. K., Prakash, C., Dixit, S., Mohammed, K. A., "Mechanical and tribological properties of aluminum-based metal-matrix composites", Materials, 15(17): 6111, (2022).

[8] Mavhungu, S. T., Akinlabi, E. T., Onitiri, M. A., Varachia, F. M., "Aluminum matrix composites for industrial use: advances and trends", Procedia Manufacturing, 7: 178-182, (2017).

[9] Kumar, A., Arafath, M. Y., Gupta, P., Kumar, D., Hussain, C. M., Jamwal, A., "Microstructural and mechano-tribological behavior of Al reinforced SiC-TiC hybrid metal matrix composite", Materials Today: Proceedings, 21: 1417-1420, (2020).

[10] Muley, A. V., Aravindan, S., Singh, I. P., "Nano and hybrid aluminum based metal matrix composites: an overview", Manufacturing Review, 2: 15, (2015).

[11] Chandel, R., Sharma, N., Bansal, S. A., "A Review on recent developments of aluminum-based hybrid composites for automotive applications", Emergent Materials, 4(5): 1243-1257, (2021).

[12] Inegbenebor, A. O., Bolu, C. A., Babalola, P. O., Inegbenebor, A. I., Fayomi, O. S. I., "Aluminum silicon carbide particulate metal matrix composite development via stir casting processing", Silicon, 10: 343-347, (2018).

[13] Zhang, L., Wang, Z., Li, Q., Wu, J., Shi, G., Qi, F., Zhou, X., "Microtopography and mechanical properties of vacuum hot pressing Al/B_4C composites", Ceramics International, 44(3): 3048-3055, (2018).

[14] Veeravalli, R. R., Nallu, R., Mohiuddin, S. M. M., "Mechanical and tribological properties of AA7075–TiC metal matrix composites under heat treated (T_6) and cast conditions", Journal of Materials Research and Technology, 5(4): 377-383, (2016).

[15] Sharma, P., Dwivedi, S. P., Sharma, R., Dabra, V., Sharma, N., "Microstructural and mechanical behavior of aluminium alloy reinforced with TiC", Materials Today: Proceedings, 25: 934-937, (2020).

[16] Reddy, M. P., Ubaid, F., Shakoor, R. A., Parande, G., Manakari, V., Mohamed, A. M. A., Gupta, M., "Effect of reinforcement concentration on the properties of hot extruded $Al-Al_2O_3$ composites synthesized through microwave sintering process", Materials Science and Engineering: A, 696: 60-69, (2017).

[17] Kutzhanov, M. K., Matveev, A. T., Narzulloev, U. U., Kuptsov, K. A., Sheveyko, A. N., Shtansky, D. V., "Microwave plasma-produced Al/Al_2O_3 microparticles as precursors for high-temperature high-strength composites", Journal of Alloys and Compounds, 972: 172879, (2024).

[18] Aktaş, S., Anıl Diler, E., "Effect of ZrO_2 nanoparticles and mechanical milling on microstructure and mechanical properties of $Al–ZrO_2$ Nanocomposites", Journal of Engineering Materials and Technology, 143(4): 041002, (2021).

[19] Abdo, H. S., Seikh, A. H., "Correlation of microstructure with compression behaviour of Al5083/ZrC nanocomposites fabricated through spark plasma sintering", Transactions of the Indian Institute of Metals, 75(9): 2273-2280, (2022).

[20] Kumar, C. A. V., Rajadurai, J. S., "Influence of Rutile (TiO_2) content on wear and microhardness characteristics of aluminium-based hybrid composites synthesized by powder metallurgy", Transactions of Nonferrous Metals Society of China, 26(1): 63-73, (2016).

[21] Chen, Y., Chung, D. D. L., "In Situ Al-TiB composite obtained by stir casting", Journal of Materials Science, 31: 311-315, (1996).

[22] Meena, K. L., Alakesh Manna., S. S. Banwait., "An analysis of mechanical properties of the developed Al/SiC-MMC's", American Journal of Mechanical Engineering, 1(1): 14-19, (2013).

[23] Karvanis, K., Fasnakis, D., Maropoulos, A., Papanikolaou, S., "Production and mechanical properties of Al-SiC metal matrix composites", In IOP Conference Series: Materials Science and Engineering, 161, 012070, (2016).

[24] Surya, M. S., Nilesh, T. V., "Synthesis and mechanical behaviour of (Al/SiC) functionally graded material using powder metallurgy technique", Materials Today: Proceedings, 18: 3501-3506, (2019).

[25] Raghuvaran, P., Baskaran, J., Aagash, C., Ganesh, A., Krishna, S. G., "Evaluation of mechanical properties of Al7075-SiC composites fabricated through stir casting technique", Materials Today: Proceedings, 45: 1914-1918, (2021).

[26] Rajasekaran, A., Pugazhenthi, R., "Study of Mechanical Properties of Stir Casted Al7075/SiCp Composites After Thermomechanical Treatment", Materials Today: Proceedings, 22: 766-771, (2020).

[27] Şimşek, İ., Şimşek, D., Özyürek, D., "The effect of different sliding speeds on wear behavior of ZrO_2 reinforcement aluminium matrix composite materials", International Advanced Researches and Engineering Journal, 4(1): 1-7, (2020).

[28] Abdizadeh, H., Baghchesara, M. A., "Investigation on mechanical properties and fracture behavior of A356 Aluminum Alloy Based ZrO_2 particle reinforced metal-matrix composites", Ceramics International, 39(2): 2045-2050, (2013).

[29] Dhandapani, C., "Characteristics on heat treatment of AA6063 aluminum extrusion based ZrO_2 molecule reinforced MMC", International Journal of Advanced Scientific Research and Management (IJASRM) 3(10): 108-113, (2018).

[30] Kumar, N., Irfan, G., "A review on tribological behaviour and mechanical properties of Al/ZrO_2 metal matrix nano composites", Materials Today: Proceedings, 38: 2649-2657, (2021).

[31] James, S. J., Ganesan, M., Santhamoorthy, P., Kuppan, P., "Development of hybrid aluminium metal matrix composite and study of property", Materials Today: Proceedings, 5(5): 13048-13054, (2018).

[32] Arif, S., Alam, M. T., Ansari, A. H., Siddiqui, M. A., Mohsin, M., "Study of mechanical and tribological behaviour of Al/SiC/ZrO_2 Hybrid composites fabricated through powder metallurgy technique", Materials Research Express, 4(7): 076511, (2017).

[33] Khan, A., Abdelrazeq, M. W., Mattli, M. R., Yusuf, M. M., Alashraf, A., Matli, P. R., Shakoor, R. A., "Structural and mechanical properties of Al-SiC-ZrO_2 nanocomposites fabricated by microwave sintering technique", Crystals, 10(10): 904, (2020).

[34] Hu, Z. Y., Zhang, Z. H., Cheng, X. W., Wang, F. C., Zhang, Y. F., Li, S. L., "A review of multi-physical fields ınduced phenomena and effects in spark plasma sintering: fundamentals and applications", Materials & Design, 191: 108662, (2020).

[35] Juliyana, S. J., Prakash, J. U., Salunkhe, S., Hussein, H. M. A., Gawade, S. R., "Mechanical characterization and microstructural analysis of hybrid composites (LM5/ZrO_2/Gr)", Crystals, 12(9): 1207, (2022).

[36] Şenel, M. C., Gürbüz, M., "Investigation on mechanical properties and microstructure of B_4C/graphene binary particles reinforced aluminum hybrid composites", Metals and Materials International, 27: 2438-2449, (2021).

[37] Abdellah, M. Y., Fadhl, B. M., Abu El-Ainin, H. M., Hassan, M. K., Backar, A. H., Mohamed, A. F., "Experimental evaluation of mechanical and tribological properties of segregated Al-Mg-Si alloy filled with alumina and silicon carbide through different types of casting molds", Metals MDPI, 13(2): 316, (2023).

[38] Uzun, A., Asikuzun, E., Gokmen, U., Cinici, H., "Vickers microhardness studies on B_4C reinforced/unreinforced foamable aluminium composites", Transactions of the Indian Institute of Metals, 71: 327-337, (2018).

[39] Asmare, A., Al-Sabur, R., Messele, E., "Experimental investigation of friction stir welding on 6061-T6 aluminum alloy using taguchi-based gra", Metals MDPI, 10(11): 1480, (2020).

[40] Tirfe, D., Woldeyohannes, A., Hunde, B., Batu, T., Geleta, E., "Investigating mechanical and physical properties of stir casted Al6061/Nano Al$_2$O$_3$/Quartz hybrid composite", Advances in Mechanical and Materials Engineering, 40(1): 189-201, (2023).

[41] Sasikumar, K., Bharathikannan, R., Raja, M., "Effect of annealing temperature on structural and electrical properties of Al/ZrO$_2$/p-Si MIS schottky diodes", Silicon, 11: 137-143, (2019).

[42] Vijayabhaskar, S., Rajmohan, T., Vignesh, T. K., Venkatakrishnan, H., "Effect of nano SiC particles on properties and characterization of Magnesium matrix nano composites", Materials Today: Proceedings, 16: 853-858, (2019).

[43] Neamati, J., "SiC and ZrO$_2$ weigh percentage effects on microstructure of al based matrix composite fabricated by spark plasma sintering method", International Journal of Advanced Engineering, Management and Science, 2(6): 239496, (2016).

[44] Yadav, M., Kumaraswamidhas, L. A., Singh, S. K., "Investigation of solid particle erosion behavior of Al-Al$_2$O$_3$ and Al-ZrO$_2$ metal matrix composites fabricated through powder metallurgy technique", Tribology International, 172: 107636, (2022).

[45] Burak, G. Ü. L., Gezici, L. U., Ayvaz, M., Çavdar, U., "The comparative study of conventional and ultra-high frequency induction sintering behavior of pure aluminum", International Advanced Researches and Engineering Journal, 4(3): 173-179, (2020).

[46] Anjaneyulu, B., Rao, G. N., Rao, K. P., "Development, mechanical and tribological characterization of Al$_2$O$_3$ reinforced ZrO$_2$ ceramic composites", Materials Today: Proceedings, 37: 584-591, (2021).

[47] Tosun, G., Kurt, M., "The porosity, microstructure, and hardness of Al-Mg composites reinforced with micro particle SiC/Al$_2$O$_3$ produced using powder metallurgy", Composites Part B: Engineering, 174: 106965, (2019).

[48] Rajasekar, M., Faizal, U. M., Sudhagar, S., Vijayakumar, P., "Influence of heat treatment on tribological behavior of Al/ZrO$_2$/fly ash hybrid composite", Materials Today: Proceedings, 45: 774-779, (2021).

[49] Al-Alimi, S. A. M., Bin Lajis, M. A., Shamsudin, S. B., Boon Long, C., "Influence of Zirconia Percent on Physical Properties of Zirconia-Aluminum Chip Matrix (Al6061) Nanocomposites", Journal of Nanostructures, 12(1): 194-203, (2022).

[50] Şenel, M. C., Üstün, M., "Dry sliding wear and friction behavior of graphene/ZrO$_2$ binary nanoparticles reinforced aluminum hybrid composites", Arabian Journal for Science and Engineering, 47(7): 9253-9269, (2022).